Supporting Information

Chen et al. 10.1073/pnas.1215834110

SI Materials and Methods

Surgical Implants. Mice were anesthetized with 1–2% isoflurane in O_2/N_2O, and injected with 0.5 μg/10 g bodyweight buprenorphine, and chronically implanted with microdrives loaded with four tetrodes. Tetrodes were constructed from HM-L coated 90% platinum/10% iridium 17-μm-diameter wire (California Fine Wire). Electrodes were aimed at the hippocampal CA1 region (1.8 mm posterior to Bregma and 0.8 mm lateral to the midline). Details of the surgical procedure had been described (1). Horseshoe-like head plates (11 mm wide × 6.5 mm long × 1 mm thick) were affixed to the frontal plate of the skull using dental cement (Kemdent). After surgery, mice were placed in a heated chamber until fully recovered from the anesthetic (normally about 1 h), and then returned to their home cages. After 1 wk of postoperative recovery, the electrodes were advanced ventrally by 60 μm/d until CA1 complex spike cells were found.

After completion of the experiments, the mice were killed with an overdose of sodium pentobarbital and perfused transcardially with saline followed by 4% paraformaldehyde. The brain was sliced coronally into 40-μm-thick sections, which were mounted and Cresyl-Violet Nissl-strained to aid visualization of the electrode tracks and tips.

Virtual Reality Set-Up. The virtual-reality (VR) system was designed for head-restrained mice on an air-cushioned spherical treadmill using adaptations to the CaveUT modification (http://publicvr.org/)* of the game engine Unreal Tournament 2004 (Epic Software). Two 24-in Samsung monitors were placed at a 90° angle arranged as in Fig. S1 to display a 3D scene generated by the VR software. The view frustum of each monitor was adjusted according its physical arrangement relative to the head, providing a single viewing location (where animals were located) from which the virtual geometry appeared undistorted. For this physical arrangement the horizontal field of view of each monitor was 83.8°, and the view was rotated by 45° in opposing directions for each monitor (note there was a "dead" space of 4° horizontal directly ahead of the animal due to the monitor bezels). Rotation of the Styrofoam ball was detected by an optical computer mouse (Razer Imperator) chosen for high resolution and sampling frequency (5,600 dots-per-inch at 1 kHz), which was positioned behind the mouse at the intersection between the equator of the ball and the medial plane of the animal. The signal at the vertical axis was interpreted by the VR software as a control signal for the forward and backward movement of the virtual location of the animal, which was logged with a resolution of 50 Hz. Reward was delivered by a syringe pump (Harvard Apparatus) attached to a silicone tube (Sani-Tech STHT-C-040-0) positioned directly in front of the mouse's mouth. The delivery of the reward was controlled by events in VR via UDP network packets to the local host captured by software written in Python 2.7 and relayed via USB to a Labjack U3 data acquisition device to produce 5v TLL signals to trigger the pump. Neural activity was recorded using the separate computer running the Axona DACQ system. Synchronization events were logged by the VR system and sent to the DACQ recordings via UDP network packets allowing virtual location to be time-locked to electrophysiological recordings.

*Jacobson J, Preussner G (2010) Visually Immersive Theater With CaveUT. World Conference on Educational Multimedia, Hypermedia & Telecommunications (ED-MEDIA2010), Toronto, Canada. Available at http://publicvr.org/. Accessed November 30, 2012.

Behavioral Procedure and Signal Recording. After postoperative recovery, the mice were placed on a food deprivation schedule with 90% of body weight. After three days of food scheduling, the mice were placed in the VR apparatus for an hour to get acclimatized to the apparatus. The head was fixed on the VR apparatus with the head plate ~25 mm above the top of the ball. After acclimatization, there were three days of training sessions in the VR apparatus. A training session on each day consisted of four trials. Trials were 10 min long, and the mice were returned to their home cages on the holding platform next to the VR apparatus between training trials (intertrial intervals were 15 min). During a trial, the mice were trained on a virtual linear track built using the UT editor, shown in Fig. S1. The virtual track was 67 cm long, measured as the number of rotations of the ball required to move from one end of the track to the other times the circumference of the ball. Five visual cues with different textures were placed on the walls of the virtual track, three on the side walls (each occupying 28% of the wall) and two on the end walls. The visual cues on the end and side walls were equally sized; they all provided about 5 lux illumination when viewed from the center of the apparatus. Two white disks on the floor at either end of the track signaled the locations where animals received reward (~5 μL soya-based infant formula milk). The mice were trained to run back and forth on the virtual track for the milk reward.

Training continued until CA1 complex spike cells were found. Probe testing session began after at least three days of training and after complex spike cells were stably recorded. A testing session normally consisted of baseline trials which used the same virtual environment as training, interleaved by six probe trials as described in Fig. S6. All trials were 6 min in duration with 15-min intertrial intervals.

Recording was made during the first 3 d of training and during the day of probe testing. Local field potentials were sampled at 250 Hz, low-pass filtered below 500 Hz, and recorded in single-ended mode. Spike signals were sampled at 48 kHz, bandpass filtered between 360 Hz and 7 kHz, and recorded in differential mode with respect to signals from a single electrode of another tetrode. Cluster cutting for isolating single units was performed manually using custom-made software (TINT; Axona).

In the real world paradigm, a 70 cm-long, 4 cm-wide linear track was made from foam board, five cue cards were attached on the wall matching the pattern in VR (Fig. S4). Mice usually had three-days experience on the linear track when recording was made. A recording session consisted of four 10-min trials with 15-min intervals, VR trials and real-world trials were alternated. Complex spike cells (n = 83) fired in both VR and real-world environments were included for comparisons.

Data Analysis. ***Firing rate maps.*** Firing rate maps were constructed as follows. Spike and position data were first separated in terms of the direction of the movement: eastwards (315°–45°) and westwards (135°–225°). Position data were sorted into 1.7 cm bins. The binned data were then individually smoothed using a Gaussian kernel over the surrounding 5 bins. Firing rates in each bin were calculated by dividing the total number of spikes during occupancy of the bin by the total duration of occupancy. The ten colors of the firing-rate maps were auto-scaled to represent 10% of the peak rate – red (top 10%) to dark blue (bottom 10%). The peak firing rate is shown next to each map.

Spatial information. Spatial information was measured on adaptive smoothed rate maps (2), and was expressed in bits/spike.

Phase precession. A place field was defined as continuous bins where firing rate was above 20% of the peak rate. Local field potentials were digitally filtered for theta (4–12 Hz). Spike phase was calculated using a Hilbert transform. In the plot of spike phase versus position, a best fit line was found using circular-linear fit (3). A linear correlation coefficient was calculated based on the phase angles unwrapped around the best fit line.

Spatial correlation. Spatial correlation was calculated by correlating rate values of spatially corresponding bins from two comparing trials, using only bins with firing rate >0 Hz in both trials.

Centroid shift. The centroid of the firing rate map was calculated as: $\sum_{i=1}^{n} x_n f(x_n) / \sum_{i=1}^{n} f(x_n)$, where $f(x_n)$is the firing rate in the bin at x_n, there were $n = 37$ bins. The centroid shift was the difference of map centroids between trials, positive shift was defined as the shifting direction against running direction.

Theta index. Theta index is defined by the ratio of the theta power (the mean power within 1 Hz around the theta peak) to the mean power in the frequency range of 2–40 Hz.

Cell categorization. To quantify the cell response to our various manipulations to the visual cues, we calculated the spatial correlations between all baseline trials, and used the Mean-2SD (r = 0.51) as a threshold for the spatial correlation between probe and baseline trials. If the correlation fell below the threshold, the probe-trial firing pattern was deemed to be significantly affected by the manipulation in that probe condition. Thus, visually dependent cells showed a spatial correlation between baseline and the no-visual-cues probe trial that fell below 0.51. Cells were deemed to depend on specific visual cues if the correlation between baseline and trials with those cues removed was below threshold. Similarly, visual information alone was deemed sufficient for cells that showed above-threshold spatial correlations between the baseline and passive movement trials, while cells with below-threshold correlations were deemed to require movement-related information as well as visual information.

We also calculated the centroid shift in all baseline trials and used the Mean-2SD (2.93 cm) as a threshold for the centroid shift between baseline and half-speed trials to identify cells whose field location shifted in half-speed trials.

1. Cacucci F, Wills TJ, Lever C, Giese KP, O'Keefe J (2007) Experience-dependent increase in CA1 place cell spatial information, but not spatial reproducibility, is dependent on the autophosphorylation of the alpha-isoform of the calcium/calmodulin-dependent protein kinase II. *J Neurosci* 27(29):7854–7859.
2. Skaggs WE, McNaughton BL, Gothard KM, Markus EJ (1993) An information-theoretic approach to deciphering the hippocampal code. *Adv Neural Inf Process Syst* 5:1030–1037.
3. Schmidt R, et al. (2009) Single-trial phase precession in the hippocampus. *J Neurosci* 29 (42):13232–13241.

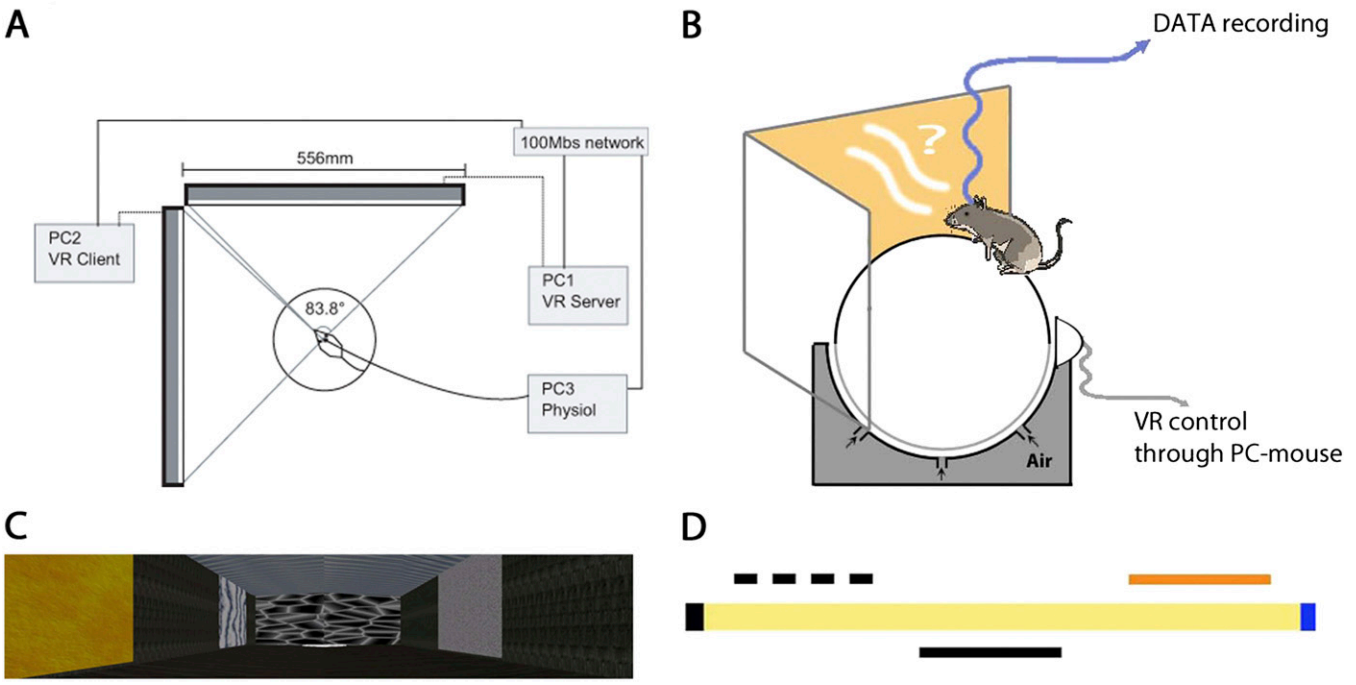

Fig. S1. (*A*) Plan view of virtual reality (VR) setup. (*B*) Mouse on air-cushioned ball. (*C*) Mouse view of VR environment. (*D*) Schematic representation of VR track (in yellow) with visual cues.

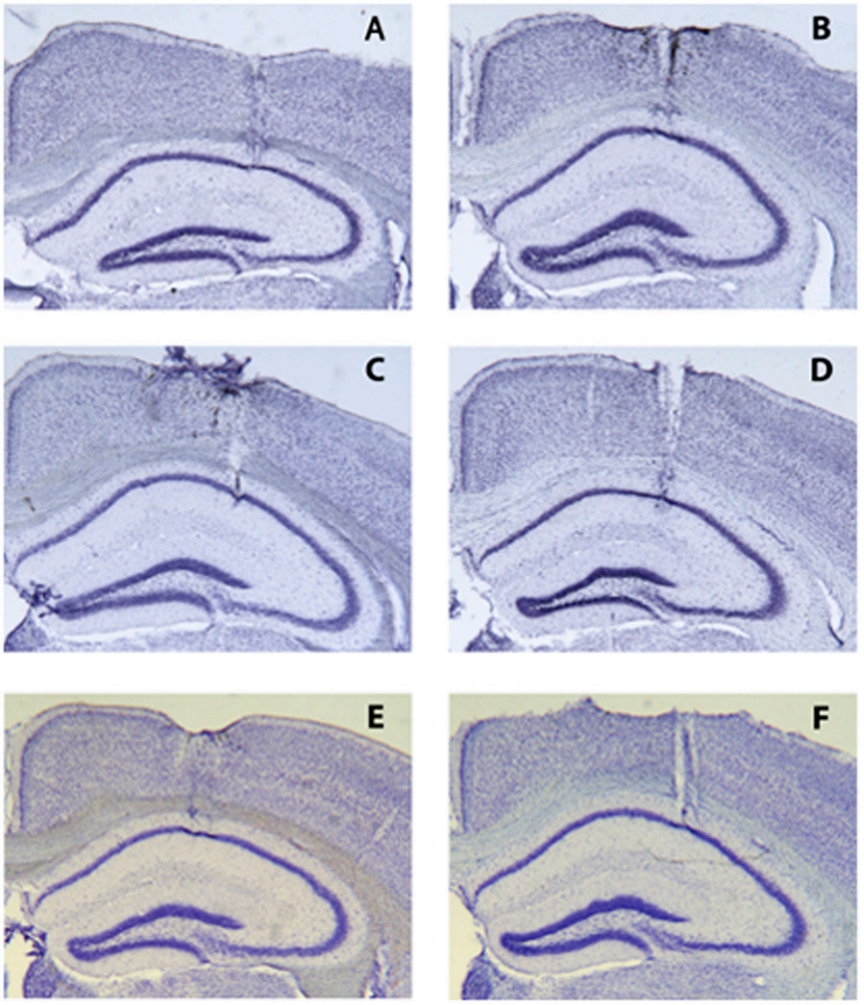

Fig. S2. Nissl-stained brain sections from 6 different rats (*A–F*) show tetrode tracks ending in the CA1 field of the hippocampus.

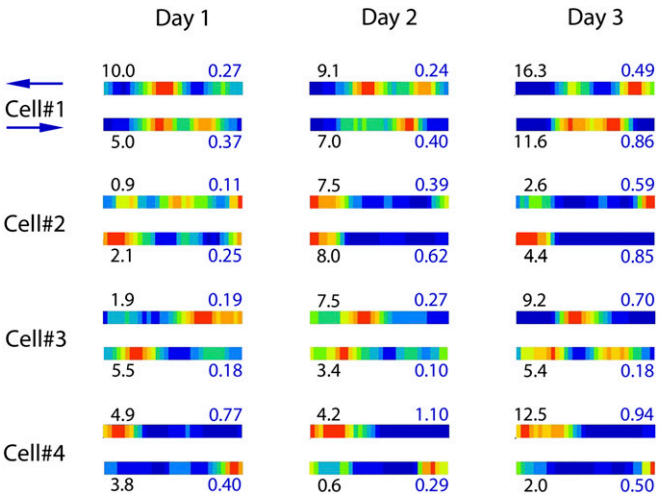

Fig. S3. Place cells on virtual reality linear track during first 3 d of training.

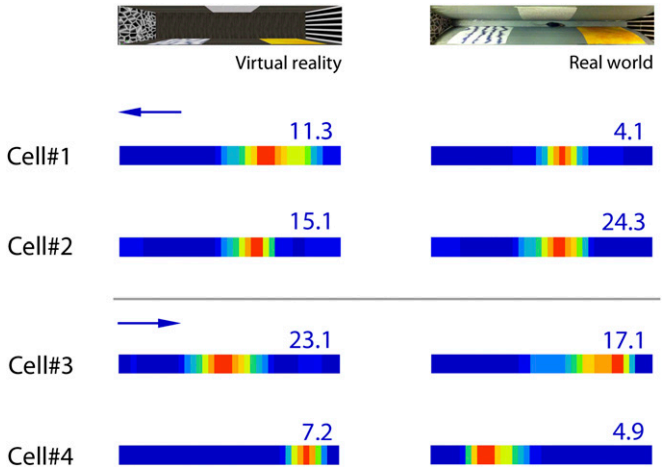

Fig. S4. Place cells on comparable linear tracks (viewed from above) in virtual reality (*Left*) and in real world (*Right*). A total of 19% of cells had fields in comparable places in the two environments (cells 1 and 2) but the majority (69%) had fields in different places (cells 3 and 4).

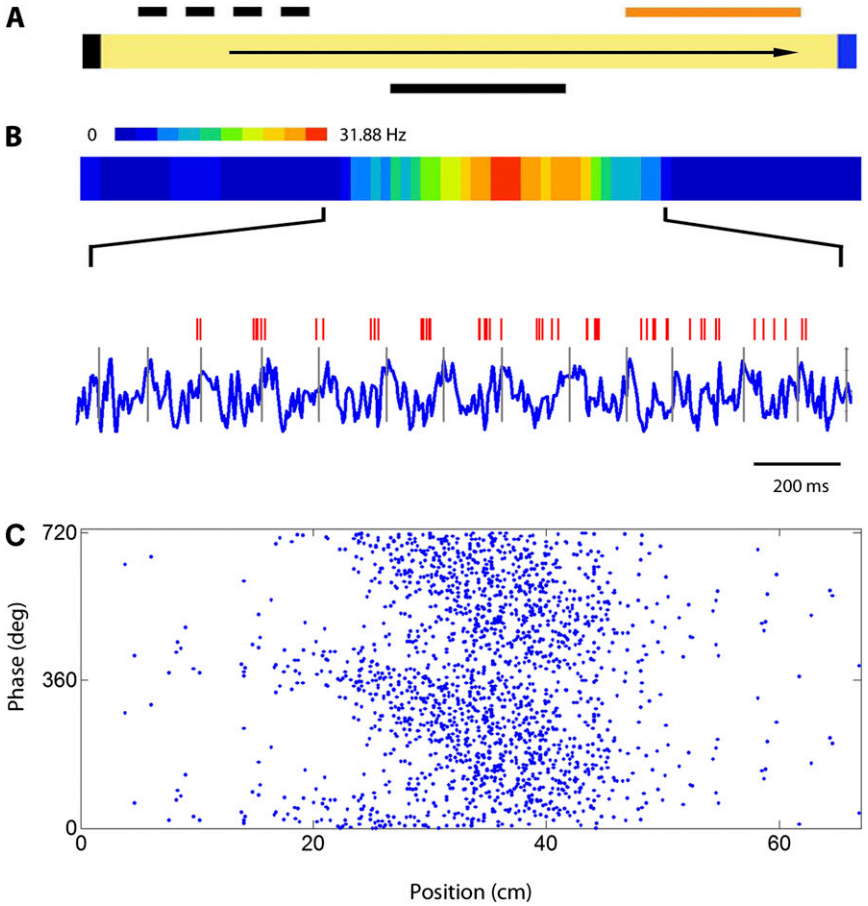

Fig. S5. A typical example of theta precession. (*A*) A schematic showing eastward runs. (*B*) Cell burst firing with each burst moving earlier on the local LFP Theta. Vertical gray bars identify troughs of waves. (*C*) Phase precession across multiple trials was correlated with position on virtual linear track (r = -0.60).

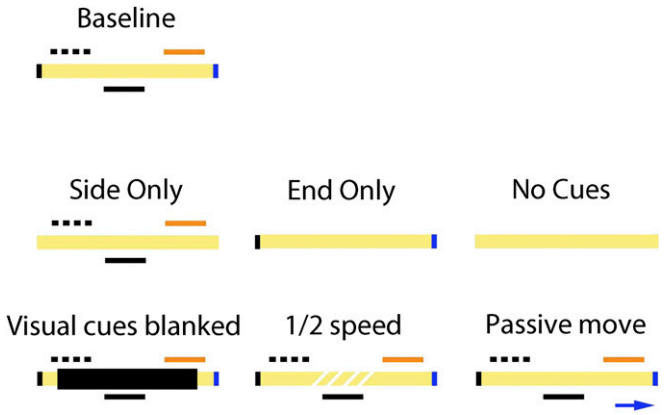

Fig. S6. Experimental manipulations.

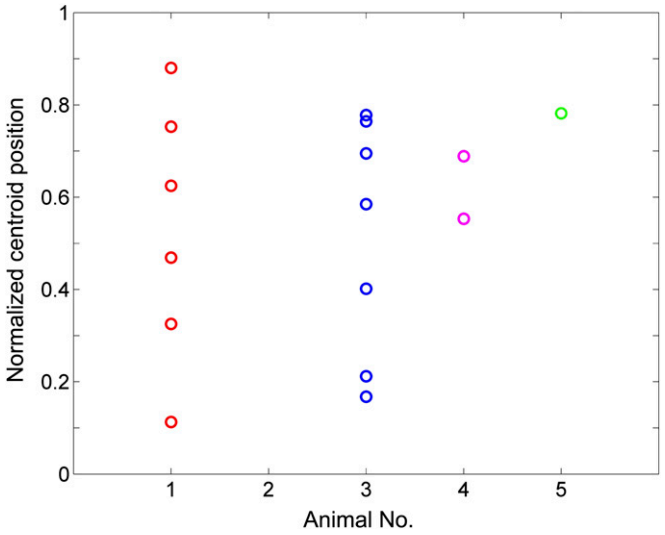

Fig. S7. Distribution of the maintained fields along the track in the passive movement trial. The fields were not clustered around the reward points at the ends of the track ($y = 0, 1$), but were distributed fairly equally across the whole track. Centroid position was normalized into 0–1. The x axis indicates the animal number. Circles in different colors indicate place fields from different animals.

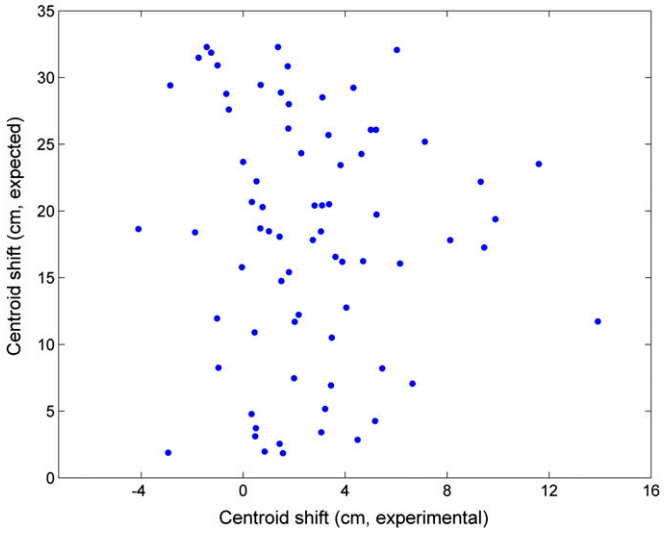

Fig. S8. No significant correlation was found ($r = 0.20$, $P = 0.11$) between the distance of the field from the start (y axis) and the amount of backward shift (x axis).